Hindawi
Advances in Civil Engineering
Volume 2023, Article ID 9689218, 16 pages
https://doi.org/10.1155/2023/9689218

Research Article

Implementation of an Advanced Macroelement Beam Model under Moving Load (Case Study: Iranian Railroad Projects)

Hamid Reza Vaziri,[1] **Mohammad Reza Mansoori**,[1] **Fereydoon Arbabi**,[2] **and Armin Aziminejad**[1]

[1]*Department of Civil Engineering, Science and Research Branch, Islamic Azad University, Tehran, Iran*
[2]*Department of Civil Engineering, Michigan Technological University, Houghton, MI, USA*

Correspondence should be addressed to Mohammad Reza Mansoori; m.mansoori@srbiau.ac.ir

Received 20 September 2022; Revised 2 December 2022; Accepted 24 March 2023; Published 26 April 2023

Academic Editor: Reza Lotfi

This study aims to present a new three-dimensional moving macroelement for the numerical analysis of beam on the elastic foundation under moving loads as a railroad track vibration. Our research is based on a case study conducted in Iranian Railroad Projects. Due to involving a large number of elements, vibration analysis of beams as railroad tracks with standard three-dimensional elements is time-consuming. Two approaches are used and combined in this research to improve analysis of realistic models. The former is to use a macroelement with a number of degrees of freedom that can be used in lieu of standard three-dimensional elements. The latter is to use moving elements to ensure that the loads do not approach the boundaries of the model, thus leading to boundary errors. Accordingly, the moving element was formulated at different velocities to allow correct evaluation of the trains' acceleration and deceleration effect. The analysis is based on a linear model. Examples with different number of elements and boundary conditions were included to evaluate the effects of the track parameters. One important aspect of the formulation is the asymmetric nature of stiffness and damping matrices due to the effects of velocity and the moving load. In the moving element method, with a sufficient number of elements, no end condition effect exists. However, because acceleration may be a more critical parameter than displacement, the number of elements must be determined for acceleration, as well. Our important achievements include formulating the interaction of lateral and torsional degrees of freedom, the possibility of calculating probable warping in the beam due to cross-sectional slenderness both directly and based on introducing a dependent degree of freedom, and also determining the model length based on vibrational acceleration at the end of the model. Besides, reduction of analysis time is a prominent feature of the present model.

1. Introduction

Vibration analysis of railroad tracks as beam models on elastic foundations under moving trains is important for both designing new tracks and operating existing ones. Many studies have examined free and forced vibration of continues beams as tracks under different loading conditions including trains moving at steady speed and while accelerating and braking, as well as temperature changes and the effects of earthquakes. The focus on trains moving on a track stems from the implications for designing and maintenance [1–6].

Fryba [3] employed a Fourier transform when examining a beam under moving loads. Fryba et al. [4] also studied a beam on a foundation having randomly varying stiffness under a moving force using the finite element technique. Chen and Huang [5] and Anderson et al. [6] studied the track as a beam model under a concentrated load and mass. The newly suggested techniques which appear to be very appropriate for railroad tracks due to moving nature of train loads include the moving coordinate method [7] and its counterpart, the moving element method [8].

The current research is based on studies of moving loads, which are relevant to the vibration of tracks under trains. For

instance, Mathews [9] most recently examined a track under a moving load in the frequency domain. Similar studies have been conducted by Jezequel [10] and Ono and Yamada [11], who modeled the rail as an infinite Euler–Bernoulli beam. Trochanis et al. [12] used a Fourier transform in order to model the rail. Calım [13] studied forced vibration of curved beams on a two-parameter elastic foundation subjected to impulsive loads. He modeled the curved beam by finite elements with two degrees of freedom (DoFs) at each node.

Dai et al. [14] analyzed an efficient numerical study on the dynamic response of a partially filled freight train subject to abrupt braking through the moving element method computationally. Nguyan and Duhamel studied the nonlinear behavior of bars [15] and beams [16] on elastic supports under harmonic moving loads. On the bar element, the velocity was assumed to be constant and linear springs were used to model a Winkler foundation, leading to the equations of motion using moving coordinate. On the beam element, the analysis was conducted under similar loading conditions and both studies were carried out in the time domain. The foundation stiffness was given a nonlinear form to make prediction of soil failure possible.

Nguyan et al. [17] analyzed the effect of a moving mass on a nonlinear foundation. Kouroussi and Verlinden [18] modeled a railroad with lumped masses to study train, track, and foundation interactions. Ferrira and López-Pita [19] studied the maintenance needs of railroad tracks through numerical modeling using Dynavoie to optimize the track designs. The finite element model was also used to consider the dynamic interaction between the train and track and all its components.

Zakeri and Xia [20] modeled the beams having infinite lengths on elastic foundations at the end of their finite element model. They showed the possible boundary conditions' effect on the dynamic response. In order to reduce such effects, the length of the track was chosen so as to minimize the dynamic responses at the end points. Because the acceleration response can propagate farther, it is important to choose a length at which acceleration is negligible at the boundaries.

Sarvestan et al. [21] studied vibration of cracked Timoshenko beams subjected to moving loads. The crack was modeled using two massless springs, leading to the dynamic stiffness matrix of the beam. Their study included both a constant velocity and a constant acceleration of moving loads. Spectral analysis was performed in the frequency domain, and the model used a two-dimensional plate element with two DoFs at each node. Uzzal et al. [22] determined the dynamic response of an Euler–Bernoulli beam subjected to moving loads as well as a moving mass supported on a two-parameter Pasternak foundation using the Fourier transform technique. Beam elements were used to simulate different structures including gas pipelines. Hua et al. [23] evaluated the dynamic behavior of an axially moving beam to study its internal pressure using the finite element method. The studied model consisted of a one-dimensional beam subjected to an internal pressure. The Newmark-β time integration method was adopted to calculate the dynamic responses of the model. Finally, effects of the internal pressure on the dynamic model of the beam were investigated. Afterwards, Mei et al. [24] studied the dynamic behavior of a long beam on an elastic foundation. A reduced time-varying model and Hamilton's principle were employed in their study. More recently, Jahangiri et al. [25] analyzed an Euler–Bernoulli beam under a moving mass with large oscillations using Galerkin and perturbation methods. They solved the problem in presence of an external harmonic force applied on the moving mass through the perturbation method. Phadke and Jaiswal [26] studied the impact of a nonhomogeneous elastic foundation on dynamic response of railway track. The track was modeled as a long beam on a nonhomogeneous elastic foundation.

Using the finite element method, Forio et al. [27] evaluated a simply supported Euler–Bernoulli elastic beam resting on a homogeneous nonlinear elastic Winkler foundation subjected to a concentrated moving load. The beam was examined at different velocities in order to determine the critical velocity at which large displacements could damage the structural elements. The authors established a relationship between the critical velocity and moving load parameters.

The moving coordinate and moving element methods are appropriate for railroad tracks with moving train loads [7, 8]. The former method provides an advantage of the form of the moving load on the rail element, where it is not necessary to determine the end conditions of the model, and thus the load effects are never experienced at the end point. Since the beam model is infinite, the upstream and downstream ends of the beam model are sufficiently far from the load points to make their effect negligible. This form of modeling is similar to that of pushing the rail under the train that each load point contact remains constant.

Koh et al. [7] showed that, in the moving element method, the elements are conceptual and move under the vehicle while it remains stationary. In this way, the relative movement of the vehicle with respect to the track is demonstrated and the train never reaches the end of the track model. Koh et al. [7] considered both smooth rails as well as corrugated ones. Tran et al. [8] continued this research by including variable velocities. In these studies, common one-dimensional beam elements were used as the moving elements. The governing equations of motion were derived using a Galerkin approach with examples primarily related to displacement in one direction. The examples included moving loads with variable velocities at a constant acceleration.

In the present study, a new macroelement and a moving coordinate system are used to evaluate the dynamic response of a beam model as the track under moving train loads. The model is three-dimensional in nature so that the response can be evaluated by considering the interaction of the displacements in different directions. Because this model can provide accurate and economical solutions, it can be used to evaluate the simultaneous effect of earthquakes and moving trains contemporarily or separately. The model can be used to simulate earthquake and train load as a moving load either simultaneously or separately. It also paves the way to

investigate the interaction of lateral and torsional DoFs in related loading cases.

Although the macroelement [28, 29] and the moving element method [7, 8] have been used by previous researchers, the current article combines the two techniques to provide an efficient means of dealing with infinite domain railroad tracks. The moving element method ensures that the effect of end conditions does not invalidate the results. In modeling the track system, the smooth rail is modeled as an Euler–Bernoulli beam resting on an elastic base. The base is represented by linear springs that can be either continuous or discrete. In numerical examples, continuous springs are generally used. The springs can also be rotational to allow modeling of rotational stiffness. The macroelement requires seven DoFs, six of which for modeling displacement and rotations in a three-dimensional coordinate along with a dependent additional DoF for modeling possible warping of the rail. Besides, due to such gaps in previous studies as follows, the current study seemed to be necessary: (1) lack of accurate modeling of rail bed, (2) impossibility of modeling and accurate investigation of bed damping, and (3) lack of providing a comprehensive model for use in curved and straight beams.

Here, the following basic problems are to be answered:

(1) Introduction of a comprehensive macroelement model for straight railway lines located on elastic bed.

(2) What are the limitations of the length of the rail? And what factors the number of model elements in modeling depend on?

(3) What is the effect of moving load parameters such as speed and acceleration as well as the amount of load on the response of the rail?

(4) What are the effects of rail interaction in different degrees of freedom?

2. Problem Statement

The symbols used in the equations are defined in Table 1.

2.1. Formulation of Macroelement. The macroelement used in this study was developed by Arbabi et al. [28–33] and proved to be an efficient model for studying unbounded domains such as railroad tracks. The element (Figure 1(a)) has two nodes with seven DoFs at each node. One, u, is related to axial deformation in the x direction, and the lateral deformations v and w are in the vertical and horizontal (y and z) directions, respectively. The rotational deformations about y and z axes are θ_z and θ_y, respectively.

Rotation about the x axis is dominant because it describes the torsional deformation. Its derivative is the warping parameter denoted by β without a subscript. In order to calculate warping, a separate DoF is denoted as β'. Figure 1 shows that the parts of the rail section below the head have much thinner sections; therefore, warping can be significant.

Since the foundation provides distributed support for the rails, distributed springs were used to model the foundation. The springs are in the vertical and horizontal directions denoted as k_y and k_z, respectively. Similar springs exist in the x direction to account for the axial stiffness of the track caused by the friction between the traverses and ballast as well as the ballast and the ground. The interaction of the ballast and railroad traverses can also provide rotational resistance against the bending of the rails. The distributed torsional spring, k_t, is provided to account for such resistance. The vertical and horizontal dashpots with coefficients c_y and c_z are provided to address damping of the track.

2.2. Rail Properties. The component properties of the numerical examples considered here are those used in Iranian railroads [34]. The properties of the cross sections of the rails, UIC-60, are presented in Figure 2 [34] and Table 2.

In McGuire et al. [35], warping constant Γ is calculated as follows:

$$\Gamma = \frac{I_y d^2}{4}, \tag{1}$$

where I_y is the second moment of area about the y axis and d is the height of the rail section. For portions of the track where the traverses are placed on concrete slabs, a concrete strength of $f_c' = 400\,\text{kg/cm}^2$ is assumed and modulus of elasticity E_c has been calculated according to the Iranian concrete code. Table 3 lists the stiffness and the dashpot properties of the railroad models.

2.3. Governing Equations for Moving Macroelements. Beams on elastic foundations are used for different engineering problems. Thus, the formulations can be one, two, or three-dimensional. The one-dimensional case under axial deformation is applied for pile-driving as well as for railroad tracks. Because of its simplicity, it is also a good problem for the demonstration of the formulation process. Metrikine and Dieterman [36] modeled a beam on a viscoelastic foundation under a mass moving in the axial direction. They assumed that the mass and the beam are in continuous contact and have a vertical constant force, respectively.

The equation of motion is found by applying the Hamilton principle, after which the coordinates change to a new moving coordinate system. The Hamilton principle leads to

$$\int_{t1}^{t2} \delta(K - \Pi)\mathrm{d}t + \int_{t1}^{t2} \delta W \mathrm{d}t = 0, \tag{2}$$

where K is the kinetic energy of the mass, Π denotes the potential energy of the beam and supports, and W is the nonconservative work of damping. The total kinetic energy can be written in terms of the kinetic energy of the moving mass plus the work of the external force.

Table 1: Symbol definition.

Symbol	Definition
u, v, w	Axial and lateral deformation in the x, y, and z directions, respectively
$\dot{u}, \dot{v}, \dot{w}$	Axial and lateral velocity in the x, y, and z directions, respectively
$\ddot{u}, \ddot{v}, \ddot{w}$	Axial and lateral acceleration in the x, y, and z directions, respectively
β	Torsion angle around x direction
β'	Warping factor definition
$\overline{k}_x, \overline{k}_y, \overline{k}_z$	Stiffness factor per unit length of the beam in the x, y, and z directions, respectively
$\overline{k}_t$	Rotational stiffness factor per unit length of the beam
$\overline{c}_x, \overline{c}_y, \overline{c}_y$	Damping factor per unit length of the beam in the x, y, and z directions, respectively
$\overline{c}_t$	Rotational damping factor per unit length of the beam
$\overline{m}$	Mass per unit length of the beam
$\overline{J}_m$	Rotational mass inertia per unit length of the beam
E	Modulus of elasticity
A	Area section
Γ	Warping factor
K	Kinetic energy
Π	Potential energy
W	Nonconservative works
ρ	Mass density
ε	Strain of beam model
I_x, I_y, I_z	The second moment of area in the x, y, and z directions, respectively
J	Second polar moment of area
h	Distance between shear center and bottom level of the rail
P, q_y, q_z	Moving point load in the x, y, and z directions, respectively
T	Concentrated rotational moment around the x axis

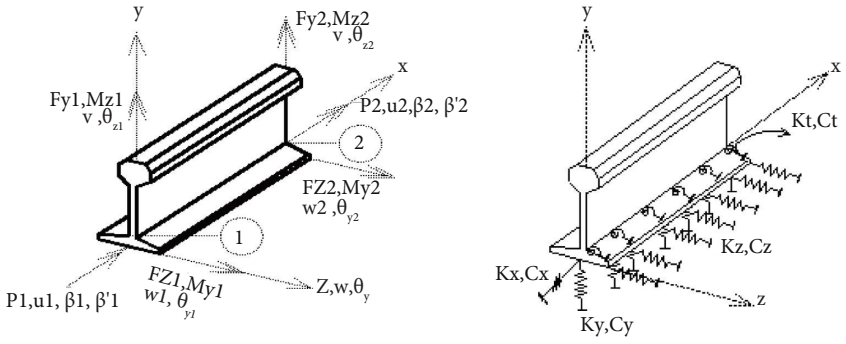

Figure 1: Rail macroelement model and DoF definitions [28].

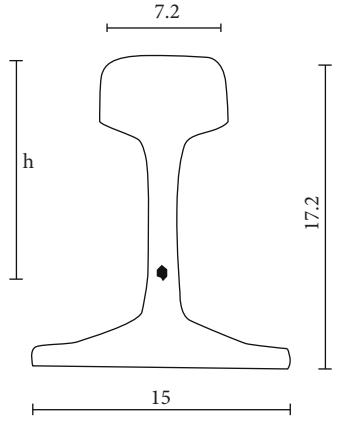

Figure 2: UIC-60 rail section (cm) [34].

Table 2: Rail section properties.

Definition	Symbol	Value
Weight per unit length	$\overline{W}$	6034 kg/m
Section area	A	7587 mm^2
Second area moment about z axis	I_z	30.55×10^6 mm^4
Second area moment about y axis	I_y	5.13×10^6 mm^4
Modulus of elasticity	E	2×10^5 MPa
Weight per unit volume	γ	7.85 ton/m^3
Warping constant [35]	Γ	3.79×10^{10} mm^6

Table 3: Spring and dashpot properties of models.

Definition	Symbol	Value
Stiffness in y direction	$\overline{k}_y$	1.00×10^7 N/m
Stiffness in z direction	$\overline{k}_Z$	1.67×10^6 N/m
Rotational stiffness	$\overline{k}_t$	4.58×10^4 (N·m)/m
Damping factor in y direction	$\overline{c}_y$	4900 (N·s)/m
Damping factor in z direction	$\overline{c}_z$	2500 (N·s)/m

2.3.1. Equilibrium Equation for Axial Deflection. The Hamilton principle for the axial deformation is defined as follows:

$$\int_{t1}^{t2} \delta\left(K_{\text{axial}} - \Pi_{\text{axial}}\right)\mathrm{d}t + \int_{t1}^{t2} \delta W_x\, t = 0, \tag{3}$$

in which

$$K_{\text{axial}} = \frac{1}{2}\int_V \rho \dot{u}^2 \mathrm{d}V, \tag{4}$$

where K_{axial} is kinetic energy in terms of axial displacement (equations (4) and (5)). By setting the mass per unit length as $\overline{m} = \rho A$ and $dV = Adx$, the last equation would be as follows:

$$K_{\text{axial}} = \frac{1}{2}\int_0^l \overline{m}\dot{u}^2 \mathrm{d}V. \tag{5}$$

The potential energy in the axial direction is defined as

$$\Pi_{\text{axial}} = \Pi_{a-i} + \Pi_{a-e} = \frac{1}{2}\int_V E\varepsilon^2 \mathrm{d}V + \frac{1}{2}\int_l \overline{k}_x u^2 \mathrm{d}x - P.u, \tag{6}$$

where Π_{a-i} is the internal potential energy due to the elastic deformation of the beam and Π_{a-e} is the potential energy of the support due to its stiffness effect and the work of external load on the model. Here, the foundation is modeled as a distributed linear spring in the x direction with stiffness $\overline{k}_x$ per unit length of the beam. Equation (3) converts to

$$\frac{1}{2}\int_0^l \overline{m}\dot{u}^2 \mathrm{d}x + \frac{1}{2}\int_0^l EAu'^2 \mathrm{d}x + \frac{1}{2}\int_0^l \overline{k}_x u^2 \mathrm{d}x + \int_0^l \delta W_x \mathrm{d}x = 0, \tag{7}$$

where ε is the axial strain and is equal to the first partial differential of u as $\varepsilon = (\partial u/\partial x) = u'$ and E is the modulus of elasticity of the beam. The nonconservative work of the axial force is

$$W_x = \int_0^l \frac{1}{2} f_{DX}(\delta u)^2 dx \Longrightarrow \delta W_x = \int_0^l f_{DX}.\delta u dx \text{ with } f_{Dx} = \overline{c}_x \dot{u}, \tag{8}$$

$$\delta W_x = -\int_0^l \overline{c}_x \dot{u}.\delta u \mathrm{d}x, \tag{9}$$

where $\overline{C}_x$ is the damping factor per unit length as shown in Figure 1(b). Following variational calculus rules, we get

$$\int_{t1}^{t2} \delta\left(\frac{\mathrm{d}u}{\mathrm{d}t}\right)\mathrm{d}t = \int_{t1}^{t2} \frac{\mathrm{d}}{\mathrm{d}t}(\delta u)\mathrm{d}t. \tag{10}$$

Through integration by parts and assuming that δu is the nonzero variation of the displacement, the statement of the Hamilton principle is

$$\overline{m}\ddot{u} + \overline{c}_x \dot{u} - EAu'' + \overline{k}_x u = p.\delta(x - Vt). \tag{11}$$

2.3.2. Equilibrium Equation for Vertical Deflection. In vertical direction y, which is the direction of the applied weight of the train and the locomotive, the process is similar to that in the axial direction. The expression of the Hamilton principle in this case is

$$\int_{t1}^{t2} \delta\left(K_{y-\text{bending}} - \Pi_{y-\text{bending}}\right)\mathrm{d}t + \int_{t1}^{t2} \delta W_y \mathrm{d}t = 0. \quad (12)$$

The expression for axial strain due to bending as derived according to the strength of materials [37] is $\varepsilon = -y\left(\partial^2 v/\partial r^2\right)$. Having this, the expression of the Hamilton principle is

$$\frac{1}{2}\int_{t1}^{t2}\int_0^l \delta\left[\left(m\dot{v}^2\right) - \left(EI_z v'' + \overline{k}_y v^2 - q_y.v\right)\right]\mathrm{d}x\,\mathrm{d}t + \int_{t1}^{t2}\int_0^l \delta\left(-\overline{c}_y \dot{v}\delta v\right)\mathrm{d}x\,\mathrm{d}t = 0. \quad (13)$$

The following substitutions can be made:

$$\Pi_y = \frac{1}{2}\int_0^l EI_z v'' dx + \frac{1}{2}\int_0^l \overline{k}_y v^2 dx - q_y v \text{ with } v'' = \frac{\partial^2 v}{\partial x^2}. \quad (14)$$

The nonconservative work of the vertical force can be substituted as

$$\delta W_y = -\int_0^l \overline{c}_y \dot{v}\delta v \mathrm{d}x, \quad (15)$$

where $\overline{C}_y$ is the vertical damping factor per unit length which accounts for damping of the soil, ballast, and traverses. After integration of the Hamilton principle in equation (12) and by setting the variation to zero, the equilibrium equation for vertical motion becomes

$$\overline{m}\frac{\partial^2 v}{\partial t^2} + \overline{c}_y\frac{\partial v}{\partial t} + \overline{k}_y v + EI_z\frac{\partial^4 v}{\partial x^4} = q_y.\delta(x - Vt). \quad (16)$$

2.3.3. Equilibrium Equation for Lateral (Horizontal) Displacement. In the lateral z direction, the resistance of the ballast against movement of the rail acts at the base of the rail. It is important that the eccentricity of this resisting force with respect to the shear center of the rail section is not ignored. The resisting force is assumed to act at the shear center, neglecting the torsional moment induced by lateral resistance. Because this force is important in the investigation of rail overturning, which is common in train derailments, eccentricity has been taken into account and can be set to zero when comparing the results of the form without the effects of the eccentricity. The remaining formulation is similar to the formulation for vertical displacement.

Figure 1(b) shows that the lateral resisting force of the ballast is $\overline{k}_z(w - \beta h)$, where h is the distance between the top of the traverses and the shear center of the rail cross section according to Figure 2, and $\overline{k}_z$ is the lateral stiffness per unit length of the track. Using the same steps as in the derivation of the equilibrium equations in the vertical direction produces the following equation:

$$\overline{m}\frac{\partial^2 w}{\partial t^2} + \overline{c}_z\frac{\partial w}{\partial t} + \overline{k}_z(w - \beta h) + EI_y\frac{\partial^4 w}{\partial x^4} = q_z.\delta(x - Vt). \quad (17)$$

The effect of torsion around the axial x axis has conditions that are similar to the calculation in the z direction. The equilibrium equation for torsion about the axis of the track (x axis) is

$$\overline{J}_m\ddot{\beta} + GJ\beta'' + \left(\overline{k}_t + \overline{k}_z h^2\right)\beta + E\Gamma\beta^{iv} - \overline{c}_t\beta + 2\overline{k}_z h w = T.\delta(x - V.t). \quad (18)$$

In all the formulations, $\delta(x - Vt)$ is a Dirac delta function that shows the effect of the moving load.

2.3.4. Moving Coordinate System. As stated earlier, when modeling a track with a moving train, a prohibitive number or elements may be needed for the track in order to eliminate the boundary effects. This makes the use of common finite elements unworkable. Even with macroelements, practical problems are time-consuming to model on most computers. This can be alleviated by use of moving coordinates and their counterpart moving elements. In this approach, the load remains stationary, but the track moves under the load. The load then will never approach the boundaries to invalidate the results because of the boundary effects.

Consider a fixed Cartesian coordinate system x-y. Assume that the load is at the middle of the track model at point O′, and the coordinate x'-y' at point O′ is not fixed but moves at speed V, which is the same as the velocity of the moving load. In addition to eliminating the boundary effects on the critical portion of the track, which is the area of application of the load, additional advantages exist for the moving coordinate system related to unbounded problems. An example is the railroad track in that the location of the load does not change and there is no need to keep track of the element upon which the load is located or to modify its properties. Once the load vector is set, it need not be updated again. In addition, multi-axle loads (trains and locomotives) can be modeled by using appropriate element lengths so that the loads act at the nodes. Referring to Figure 3, the relation

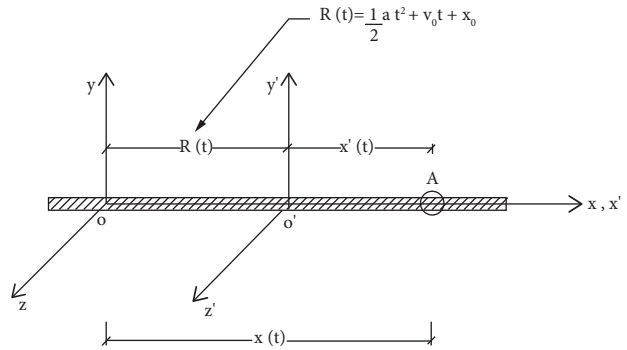

Figure 3: Moving coordinates and relationships for Cartesian coordinates.

between the old (fixed) and new (moving) coordinate systems is presented in equations (19) and (20), respectively:

$$\frac{\partial}{\partial t} \longrightarrow \frac{\partial}{\partial t} - B\frac{\partial}{\partial x^{'}(t)}, \tag{19}$$

$$\frac{\partial^2}{\partial t^2} \longrightarrow \frac{\partial^2}{\partial t^2} - a\frac{\partial}{\partial x^{'}(t)} - 2B\frac{\partial^2}{\partial x^{'}(t)\partial t} + B^2\frac{\partial^2}{\partial x^{'}(t)^2}, \tag{20}$$

where a is the constant acceleration of the load, $B = at + V_0$ in which V_0 is the velocity of the moving load, and t is time. Here, the train motion is considered to have variable velocity but constant acceleration. This allows for the investigation of trains moving at constant speed as well as accelerating and decelerating trains near the stations. For simplicity, this is written as $r = x^{'}(t)$. Equations (12), (17), (18), and (19) in the new coordinate system take the form of equations (21)–(24), respectively:

$$\overline{m}\left(\frac{\partial^2 u}{\partial t^2} - a\frac{\partial u}{\partial t} - 2B\frac{\partial^2 u}{\partial r\partial t} + B^2\frac{\partial^2 u}{\partial r^2}\right) + \overline{c}_x\left(\frac{\partial u}{\partial t} - B\frac{\partial u}{\partial r}\right) + \overline{k}_x u - EA\frac{\partial^2 u}{\partial r^2} - P.\delta(r + x_0) = 0, \tag{21}$$

$$\overline{m}\left(\frac{\partial^2 v}{\partial t^2} - a\frac{\partial v}{\partial t} - 2B\frac{\partial^2 v}{\partial r\partial t} + B^2\frac{\partial^2 v}{\partial r^2}\right) + \overline{c}_y\left(\frac{\partial v}{\partial t} - B\frac{\partial v}{\partial r}\right) + \overline{k}_y v - EI_z\frac{\partial^4 v}{\partial r^4} - q_y.\delta(r + x_0) = 0, \tag{22}$$

$$\overline{m}\left(\frac{\partial^2 w}{\partial t^2} - a\frac{\partial w}{\partial t} - 2B\frac{\partial^2 w}{\partial r\partial t} + B^2\frac{\partial^2 w}{\partial r^2}\right) + \overline{c}_z\left(\frac{\partial w}{\partial t} - B\frac{\partial w}{\partial r}\right) + \overline{k}_z(w - \beta h) - EI_y\frac{\partial^4 w}{\partial r^4} - q_z.\delta(r + x_0) = 0, \tag{23}$$

$$\overline{J}_m\left(\frac{\partial^2 \beta}{\partial t^2} - a\frac{\partial \beta}{\partial t} - 2B\frac{\partial^2 \beta}{\partial r\partial t} + B^2\frac{\partial^2 \beta}{\partial r^2}\right) + \overline{c}_t\left(\frac{\partial \beta}{\partial t} - B\frac{\partial \beta}{\partial r}\right) + \left(\overline{k}_t + \overline{k}_z h^2\right)\beta - E\Gamma\frac{\partial^4 \beta}{\partial r^4} - 2\overline{k}_z h w - T.\delta(r + x_0) = 0. \tag{24}$$

2.3.5. Finite Element Formulation. These equations can be cast in finite element form with the standard process. Because the formulations in equations (21)–(24) are in the moving coordinate system, the results would be moving elements. In this case, instead of moving, the load will remain stationary while the elements under it move to produce the relative movement of the track and train. This begins by expressing the displacement of an arbitrary point in terms of nodal displacements by employing the standard shape functions for a beam element as

$$X = \sum NS, \tag{25}$$

where X denotes a vector such as $u.v.w.\beta$ which is known as the deformation vector. For macroelement deformation, the shape functions are

$$N_u = Nu_{1\times 14}, N_v = Nv_{1\times 14}, N_w = Nw_{1\times 14}, N_\beta = N\beta_{1\times 14}, \tag{26}$$

where $Nu_{1.1} = x/l$ and $Nu_{1.8} = 1 - x/l$ and the other matrix elements of the shape function for axial deformation are equal to zero. For vertical and lateral deformations, as well as torsion, the shape function is the same:

$$N = [N1 \;\; N2 \;\; N3 \;\; N4], \tag{27}$$

where

$$N1 = \frac{2x^3}{l^3} - \frac{3x^2}{l^2} + 1, \tag{28}$$

$$N2 = \frac{x^3}{l^2} - \frac{2x^2}{l} + x, \tag{29}$$

$$N3 = -\frac{2x^3}{l^3} + \frac{3x^2}{l^2}, \tag{30}$$

$$N4 = \frac{x^3}{l^2} - \frac{x^2}{l}. \tag{31}$$

In the macroelement, the degrees of freedom are defined in Figure 1(a), with the shape functions as $Nv_{1.2} = N1$, $Nv_{1.3} = N2$, $Nv_{1.9} = N3$, and $Nv_{1.10} = N4$ as well as $Nw_{1.4} = N1$, $Nw_{1.5} = N2$, $Nw_{1.11} = N3$, and $Nw_{1.12} = N4$. For the torsion DoFs, the elements of shape function matrix can be defined as $N\beta_{1.6} = N1$, $N\beta_{1.7} = N2$, $N\beta_{1.13} = N3$, and $N\beta_{1.14} = N4$. The other elements of the shape function are zero. The pertinent matrices for the mass, stiffness, and damping in terms of the shape functions are as follows.

For the mass matrix equation:

$$M_u = \overline{m}\int_0^l N_u^T N_u \mathrm{d}r, \tag{32}$$

$$M_v = \overline{m}\int_0^l N_v^T N_v \mathrm{d}r, \tag{33}$$

$$M_w = \overline{m}\int_0^l N_w^T N_w \mathrm{d}r, \tag{34}$$

$$M_\beta = \overline{J}_m \int_0^l N_\beta^T N_\beta \mathrm{d}r, \tag{35}$$

$$M_u = M_u + M_v + M_w + M_{\beta.} \tag{36}$$

For the stiffness matrix equations:

$$K_u = \overline{k}_x \int_0^l N_u^T N_u \mathrm{d}r - \left(EA + \overline{m}B^2\right)\int_0^l \frac{\partial N_u^T}{\partial r}\frac{\partial N_u}{\partial r}\mathrm{d}r - \left(\overline{m}a + B\overline{c}_x\right)\int_0^l N_u^T \frac{\partial N_u}{\partial r}\mathrm{d}r, \tag{37}$$

$$K_v = \overline{k}_y \int_0^l N_v^T N_v \mathrm{d}r + EI_z \int_0^l \frac{\partial^2 N_v^T}{\partial r^2}\frac{\partial^2 N_v}{\partial r^2}\mathrm{d}r + \overline{m}B^2 \int_0^l N_v^T \frac{\partial^2 N_v}{\partial r^2}\mathrm{d}r - \left(\overline{m}a + B\overline{c}_y\right)\int_0^l N_v^T \frac{\partial N_v}{\partial r}\mathrm{d}r, \tag{38}$$

$$\begin{aligned} K_w = {} & \overline{k}_z \int_0^l N_w^T N_w \mathrm{d}r + EI_y \int_0^l \frac{\partial^2 N_w^T}{\partial r^2}\frac{\partial^2 N_w}{\partial r^2}\mathrm{d}r + \overline{m}B^2 \int_0^l N_w^T \frac{\partial^2 N_w}{\partial r^2}\mathrm{d}r - \left(\overline{m}a + B\overline{c}_z\right)\int_0^l N_w^T \frac{\partial N_w}{\partial r}\mathrm{d}r \\ & - h\overline{k}_z \int_0^l N_w^T N_\beta \mathrm{d}r, \end{aligned} \tag{39}$$

$$\begin{aligned} K_\beta = {} & \left(\overline{k}_t + \overline{k}_z h^2\right)\int_0^l N_\beta^T N_\beta \mathrm{d}r + E\Gamma \int_0^l \frac{\partial^2 N_\beta^T}{\partial r^2}\frac{\partial^2 N_\beta}{\partial r^2}\mathrm{d}r + \left(GJ + B^2\overline{J}_m\right)\int_0^l N_\beta^T \frac{\partial^2 N_\beta}{\partial r^2}\mathrm{d}r \\ & - \left(a\overline{J}_m + B\overline{c}_t\right)\int_0^l N_\beta^T \frac{\partial N_\beta}{\partial r}\mathrm{d}r - 2\overline{k}_z h \int_0^l N_\beta^T N_w \mathrm{d}r, \end{aligned} \tag{40}$$

$$K_e = K_u + K_v + K_w + K_\beta. \tag{41}$$

Also, for the damping matrix equations:

$$C_u = \overline{c}_x \int_0^l N_u^T N_u \mathrm{d}r - 2\overline{m}B\int_0^l N_u^T \frac{\partial N_u}{\partial r}\mathrm{d}r, \tag{42}$$

$$C_v = \overline{c}_y \int_0^l N_v^T N_v \mathrm{d}r - 2\overline{m}B\int_0^l N_v^T \frac{\partial N_v}{\partial r}\mathrm{d}r, \tag{43}$$

$$C_w = \overline{c}_z \int_0^l N_w^T N_w \mathrm{d}r - 2\overline{m}B\int_0^l N_w^T \frac{\partial N_w}{\partial r}\mathrm{d}r, \tag{44}$$

$$C_\beta = \overline{c}_t \int_0^l N_\beta^T N_\beta \mathrm{d}r - 2\overline{m}B\int_0^l N_\beta^T \frac{\partial N_\beta}{\partial r}\mathrm{d}r, \tag{45}$$

$$C_e = C_u + C_v + C_w + C_\beta. \tag{46}$$

The inclusion of velocity V and acceleration a in the formulation causes the stiffness and damping matrices to be asymmetric.

According to equations (39) and (40), it is obvious that the rail interacts with the lateral and the torsional deflections. This is because of the traverses' locations which are under the rail and do not contact the shear forces. The traverses have a distance equal to h from the shear center of the rail. This eccentricity affects the stiffness matrix, not the mass and damping matrices. It can be shown by $(-h\overline{k}_z \int_0^l N_w^T N_\beta \mathrm{d}r)$ parameter in the K_w formulation and by $((\overline{k}_t + \overline{k}_z h^2)\int_0^l N_\beta^T N_\beta \mathrm{d}r - 2\overline{k}_z h \int_0^l N_\beta^T N_w \mathrm{d}r)$ parameter in the K_β formulation. This is so important in the earthquake calculation which determines the effect of the lateral and torsional deflection modes on rail response.

3. Numerical Results

Using the formulation described here, the numerical solution was carried out in a mathematical program for the case of constant acceleration using the Newmark β method taking $\Delta t = 0{\bullet}001s$. Since similar studies have been done just in vertical direction by Koh et al. [7] and Tran et al. [8] using moving elements, the first numerical examples were compared with their results to verify the developed formulations. They used common finite elements; therefore, comparison can establish the validity and effectiveness of the macroelement used in the present study.

Figure 4(a) shows the deflected shape of the track as a beam model obtained by Koh [7] and that for the current study using the same track properties. The results were in good agreement.

According to Figure 4(b), displacement tends to zero in a very short distance away from the point of application of the force. However, in a small length of the rail, this value is

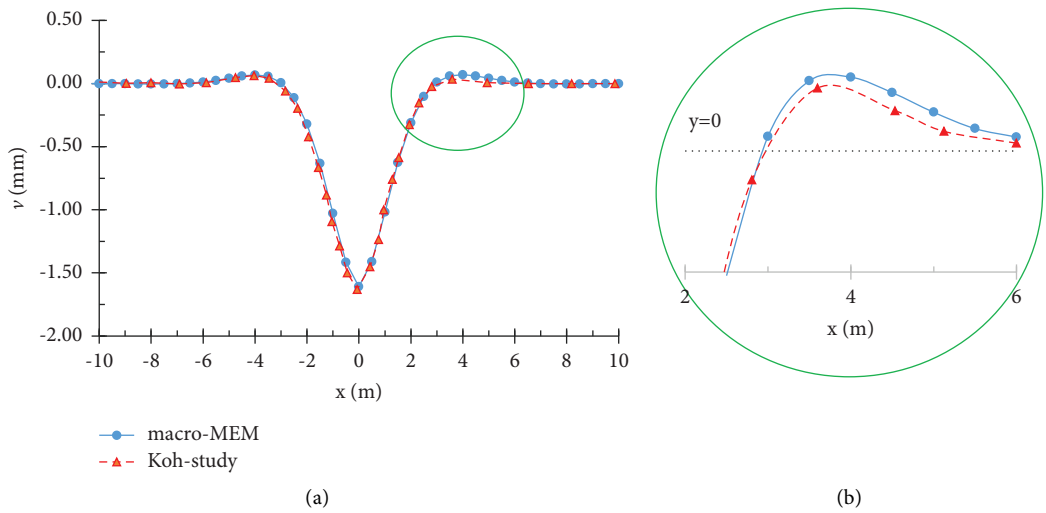

Figure 4: Verification of rail deflection under concentrated load with Koh's study [7].

set positive which can be attributed to occurrence of a weak uplift in the rail structure.

In Figure 5, the effect of two wagons with moving loads (2 concentrated loads at each wagon) on the railroad is evaluated. Interaction effect of the loads can readily be compared to the model with a single concentrated load.

Determining the correct dimension of the model is important for infinite domains so that the boundary effects do not invalidate the results. These dimensions are usually established by trial and error. The use of moving elements ensures that the load (moving train) will never approach the boundaries. However, the response of the loads applied at points on the track that are distant from the boundary must be negligible at the latter point. To ensure this, the length of the track must be determined in a way that the displacement response, velocity, and acceleration response will be negligible at the boundary. In order to avoid the shock of an abrupt load, the constant axial load is applied gradually from zero to its maximum value over a time span of one second, after which the load remains constant.

In Figure 6, the effect of boundary conditions on acceleration response of the railroad can obviously be seen. Although boundary conditions do not affect displacement response of the railroad when using the moving coordinate method, their impact on acceleration response cannot be neglected.

Figure 7 shows the velocity and acceleration of the track vibration at the end of the load period. These graphs were prepared for a constant track velocity of 80 km/h. For different ranges of train speed, the maximum velocity and acceleration of the track vibration occur in a 0.07 to 0.35 length of track at the midpoint and in a time span of 0.4 to 0.6 of the total loading time. The distance of the points, where the maximum velocity and acceleration occur, increases in front of the location of the load with the increasing speed of the train (as the train speed increases, the point experiencing maximum vibration velocity and acceleration is at a distance from the load point). This happens because of the decrease in interference by waves at high train speeds.

Train speed is a major parameter affecting the response of the track and is important in track design and maintenance. On Iranian lines, this speed is usually 80 km/h for freight trains and 100 to 160 km/h for passenger trains. For high-speed trains, the speed is usually over 200 km/h. In the current study, the speed varied from 80 to 300 km/h to demonstrate the full range of this parameter. For fast moving trains, the tracks have higher strength, which must be reflected in the track properties.

Figure 8 shows the effect of train speed on the response of the track. This graph shows the maximum response at the midpoint of the track under the point load. The maximum vibration velocity and acceleration at the midpoint occur at $t = 0.06$ to 1.0 s during load passing at different velocities. Figure 8(a) shows that an increase in train speed which had little effect on the maximum deflection of the track, but caused decreases in the track vibration velocity and acceleration, occurred in response to the effect of the moving load. The effect of train velocity on the track vibration response is shown in Figures 8(b) and 8(c).

Because the response of the track is affected by the speed of the train, it is necessary to choose an appropriate length for the model. Figure 9 shows the response at the boundary of the model for different train speeds. It is evident that dampening the effect of acceleration at the boundary is more difficult. Figure 9(a) shows that the track deflection for each length analyzed will fall to zero at the boundary points; however, the vibration velocity and acceleration of the track do not (Figures 9(b) and 9(c)). Since at the points where the displacement is equal to zero and assumed as the end point, the rail still has vibrational acceleration, the length of the computational model should be determined by the acceleration status of the end point of the model and not by the displacement of this point. The best track length for dampening of the vibration acceleration at the boundary points is over 350 m, where both the acceleration and velocity fall to zero. To model the boundary conditions of the rail, it is more effective to use springs at the boundary points that have

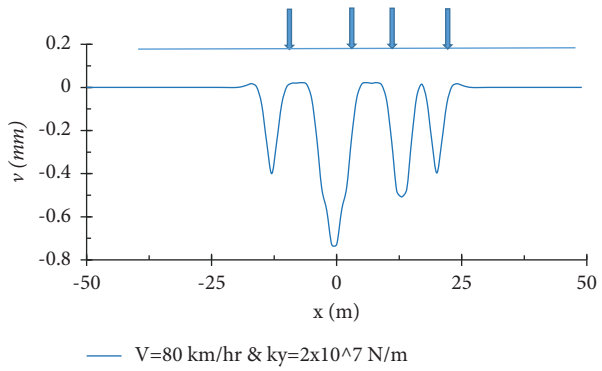

Figure 5: Rail deflection response under two wagons simulated by point loads.

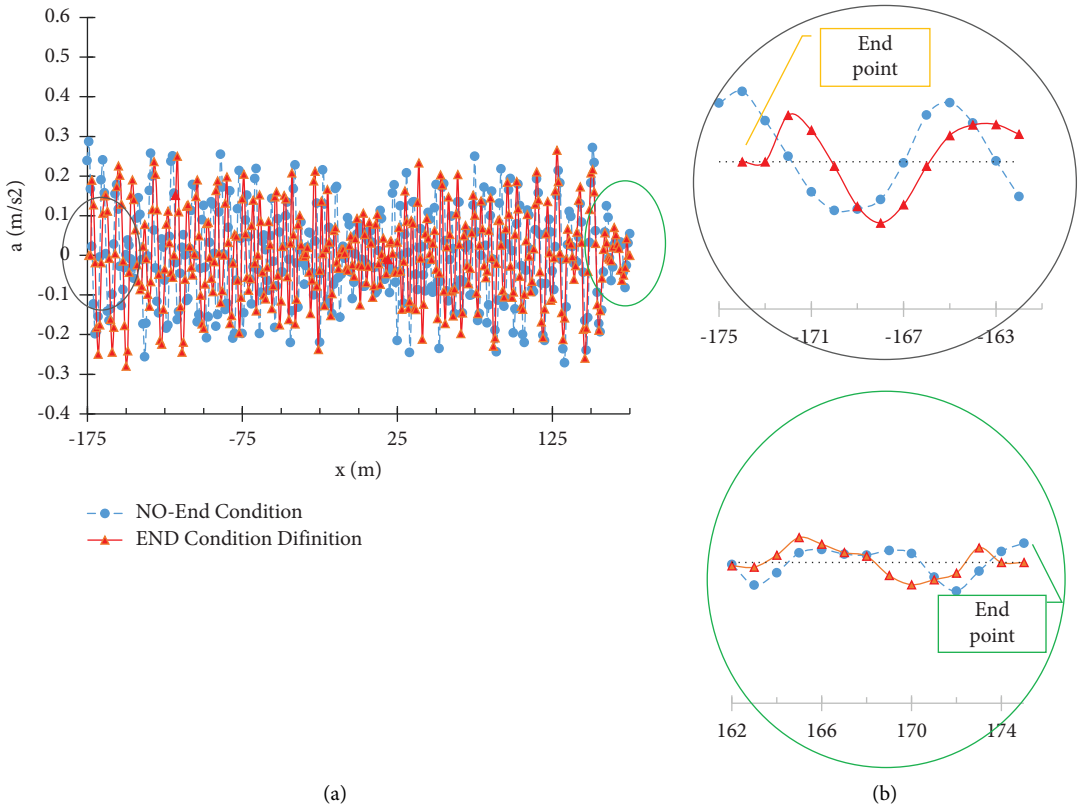

Figure 6: Comparison of acceleration response with definition of boundary conditions.

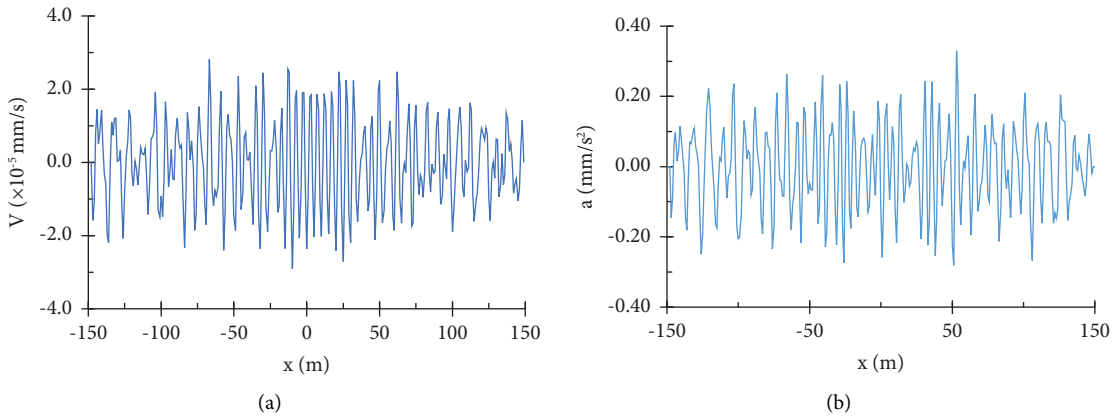

Figure 7: Track velocity and acceleration vibrational response for train velocity = 80 km/hr. (a) Velocity. (b) Acceleration.

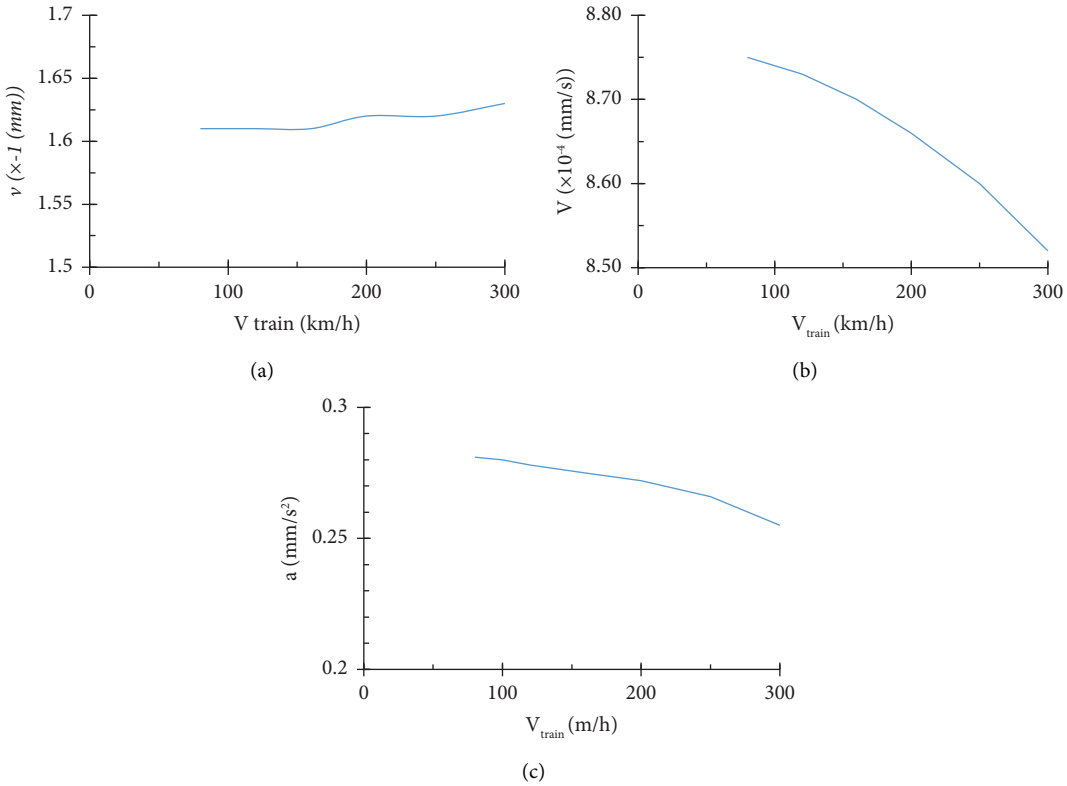

Figure 8: Response at midpoint of the track for different train speeds: (a) track max vertical deflection; (b) track max vertical velocity; (c) track vertical acceleration.

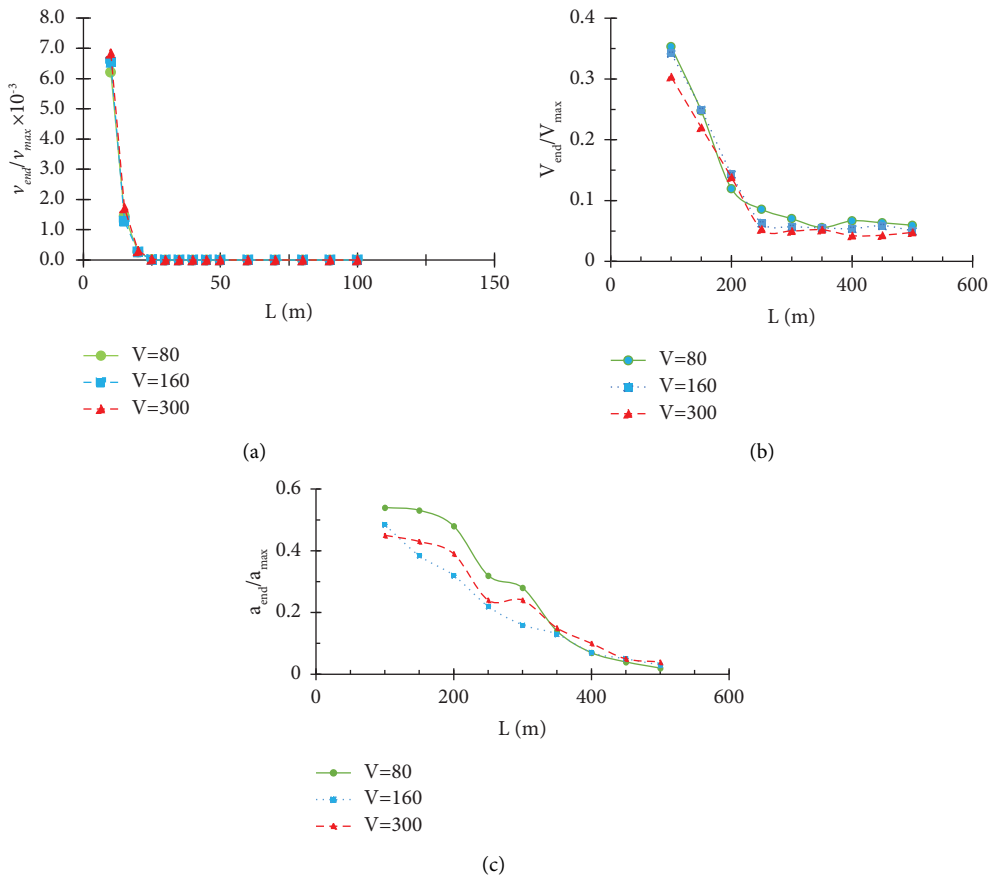

Figure 9: Ratio of end response to maximum response of the beam model. (a) Deflection. (b) Velocity. (c) Acceleration.

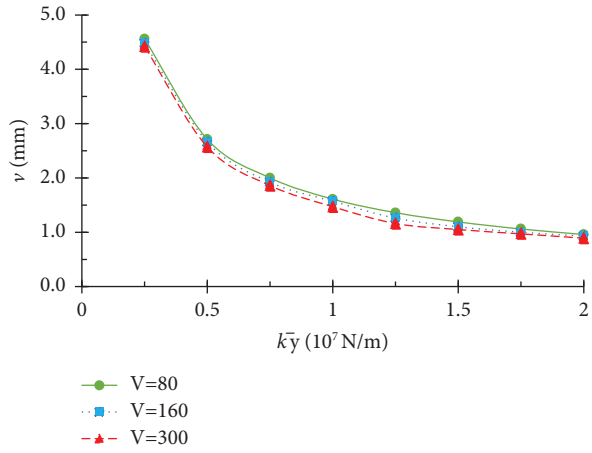

Figure 10: Midpoint deflection of rail vs. bed stiffness.

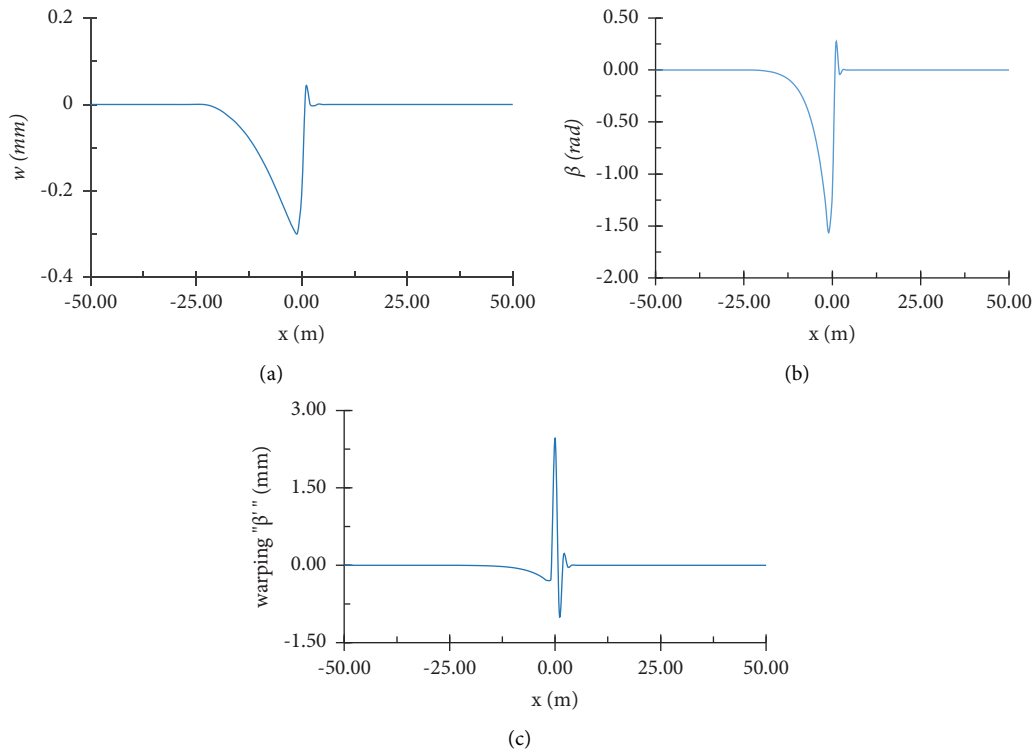

Figure 11: Track lateral deflection rotation angle and warping value response for moving lateral concentrated load velocity = 80 km/hr. (a) Track lateral deflection. (b) Track rotation angle. (c) Track warping value.

a stiffness equivalent to that of semi-infinite beam. The boundary response under such conditions is more accurate than for other forms, such as for fixing the boundary points or lack of definition of the boundaries.

Figure 10 shows the effect of the rail bed stiffness on deflection of the rail at different velocities. The bed stiffness varied from $\overline{k} = 0.25 \times 10^7 N/\text{m}$ for a soft bed to $\overline{k} = 2.0 \times 10^7 N/\text{m}$ for the hardest bed. The rate of variation of deflection of the railroad under the point load at $\overline{k} \geq 1.25 \times 10^7 N/\text{m}$ decreased more slowly than that under soft bed conditions. It was also independent of load velocity, as shown in Figure 8(a). As stated, a change in train velocity had no effect on the deflection response of the track. The deflection of the track depended on the bed stiffness as the external condition and rail properties as the internal parameters of the model.

The interaction of lateral degree of freedom along Z and the torsion and warping created in the model due to the eccentricity of stiffness and shear centers are of the most important modes in studying the vibration diagrams of a beam on elastic foundation which is also mentioned in the formulation. In order to investigate the governing

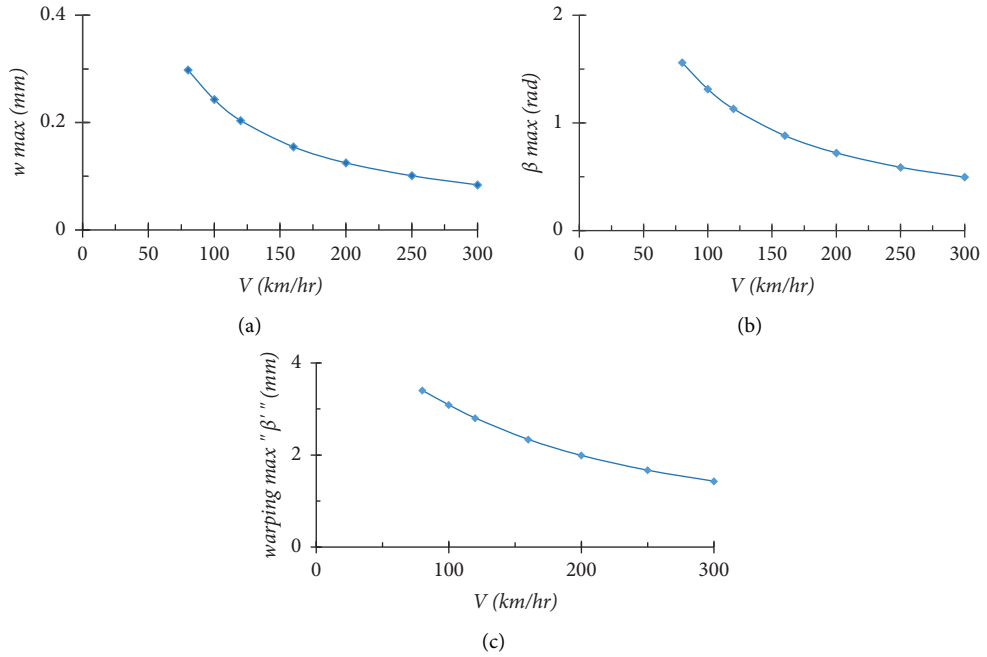

FIGURE 12: Track maximum response in the separate DoFs in the midpoint under moving lateral concentrated load with different velocities. (a) Maximum lateral deflection. (b) Maximum rotational angle. (c) Maximum warping value.

interaction conditions of the modeled beam, a concentrated force $F = 6 \times 10^3\, Kg$ is applied to the midpoint of the rail. Figures 11 and 12 examine the interactional response of the rail in the degrees of freedom related to lateral displacement, torsion, and warping due to the presence of coupled stiffness matrices. According to equations (39) and (40), by applying force in the lateral degree of freedom, w, the values of torsion and warping along the rail can be attained. The length of the rail beam is modeled to be above 200 meters to investigate the interaction of lateral and torsional degrees of freedom. Also, the speed of the lateral concentrated load on the rail is assumed to be similar to the speeds required for the vertical mode. In the results, only the diagram for a part of the rail with a significant vibration amplitude is shown. The diagrams of Figure 11 show the changes in lateral displacement, torsion angle, and warping of the rail beam model. In these diagrams, the concentrated lateral load's speed is assumed to be 80 km/hr. According to the diagrams, the maximum lateral displacement of 0.3 mm, the maximum torsion angle of 1.57 radians, and the maximum warping on the rail equal to 2.46 mm were observed for the speed of 80 km/hr. Also, the changes in the values of lateral displacement, torsion, and warping of the rail beam model for different load speeds are presented in Figure 12. Besides, the reduction of the parameters with the increased concentrated moving load's speed can be seen clearly. In the calculations related to the involved degrees of freedom in question, the changes of stiffness in different modes are not considered.

Regarding the dynamic impact of a train on the railroad, it can be simulated as a sinusoidal harmonic load with different dynamic frequencies. Thus, the frequency of the load can be considered as a variable in the analysis. The general form of the equation is (see Figure 13)

$$P(t) = P_0 \sin(\omega t). \tag{47}$$

Dynamic amplification factor (DAF) is considered as a fundamental parameter in vibration analysis of the railroads. Herein, DAF is defined as the ratio of the maximum dynamic deformation to maximum static deformation in the point of application of the concentrated force.

According to Figure 14, dynamic amplification factor is maximal for the load with vibration frequency of $\omega = 2.5$. Consequently, it can lead to resonance in the vibration of the rail. Besides, increasing the load frequency results in a decrease in DAF. Here, calculation was performed at the point of application of the force.

In order to investigate the effect of bed stiffness on DAF, AR index is defined as follows:

$$AR = \left| \frac{DAF_{\overline{k}_y} - DAF_{\overline{k}_{y=1\times10^7}}}{DAF_{\overline{k}_{y=1\times10^7}}} \times 100 \right|, \tag{48}$$

where DAF_{ky} is the equivalent dynamic amplification factor of k_y and $DAF_{ky=1\text{x}10^7}$ is the equivalent dynamic amplification of $K_y = 1 \times 10^7\, N/m$, which was used as the base value of the bed stiffness in the previous studies [7].

Figure 15 shows AR variation vs. bed stiffness for three different harmonic load frequencies. As it can be observed, the ratio is maximal when $\overline{k}_y = 0 \cdot 35 \times 10^7 N/m$ and it can be interpreted as occurring resonance in the vibrational response of the rail.

Since the acceleration of the motion of load has no significant effect on the vibrational results of the model [8], in the numerical results of this study, the results of concentrated load acceleration are considered equal to zero. Also, due to the general similarity of the formulations in

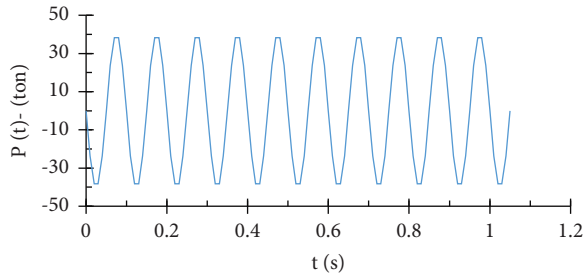

Figure 13: Harmonic load graph.

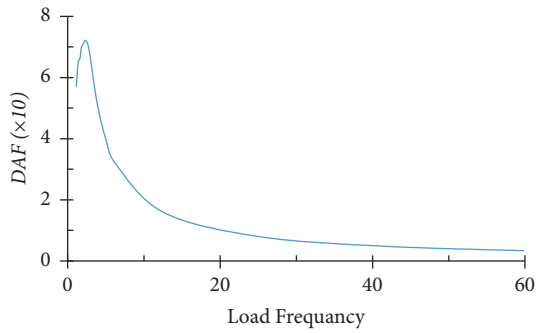

Figure 14: Railroad dynamic amplification factor due to different frequencies of the harmonic load.

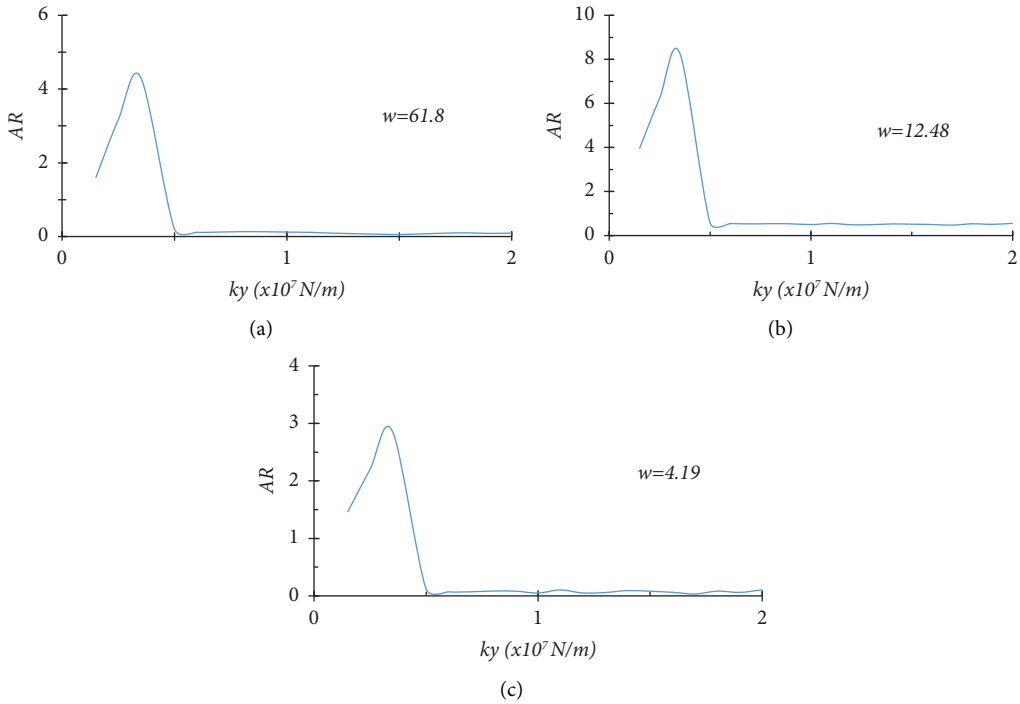

Figure 15: Variation rate of the DAF (AR parameter) vs. bed stiffness.

different DoFs, only the effective parameters in the numerical results related to the two vertical directions and the effect of the lateral point load on the lateral response of the system and the torsion angle as well as warping DoF were evaluated.

4. Motivation and Contribution

The most important motivation in this research is to create a comprehensive model to analyze the beam on the elastic bed under the effect of moving loads. One of the basic factors in modeling is examining the interaction of degrees of freedom for simultaneous analysis of loads. The most important advantage of the current model is the significant reduction in calculation time, which allows to use the characteristic matrices obtained in the results by commercial software.

5. Managerial Insight

The macroelement introduced in this article dose not have the ability to be used in the arch, and thus the relevant formulation should be modified in this context. Also, if there is a departure from the center of the load with respect to the y axis, its effect should be considered manually. Another shortcoming of the current model is the lack of investigation of nonlinear effects in the soil under the model and in the rail track itself, which are recommended to be investigated in future research and to develop the current model. For the next research, the effects of rail corrugation and the geometric nonlinearity effects of the model as well as the effects of soil interaction and soil paste conditions are suggested to be investigated. Therefore, the project managers in railroad construction can take advantage of our findings to make their plans more viable.

6. Conclusion

We aimed to introduce and develop a macroelement model for analyzing structures under the influence of moving load and relying on railroad structure. For this purpose, with the help of the moving element, the response of the rail structure was studied. The formulation was regulated based on the minimum potential energy and Galerkin method, and stiffness, mass, and damping matrices for moving macroelements were formed accordingly. Some of the matrices became asymmetric due to the speed of the concentrated load (train). The Newmark β numerical method was adopted to analyze the results in medium acceleration mode. The parameters studied in this regard are length of the model, effect of train speed, and also the rail response to lateral point load to evaluate the capability of the model.

In this study, in order to evaluate the effect of passenger and freight trains according to the conditions of Iranian trains, different train speeds are considered. The important achievement of this research is the direct relationship between the length and boundary conditions of the computational model and the vibrational acceleration of the beam model.

The vibrational responses of rails including displacement, velocity, and vibrational acceleration depend on the environmental conditions of the model, such as bed conditions, material properties, and rail cross-sectional characteristics. The interaction of the lateral transitional and torsional degree of freedom and consequent warping is amongst the other findings of this study, which is very important in seismic evaluation of rails.

Data Availability

The data used to support the findings of this study are available from the corresponding author upon request.

Conflicts of Interest

The authors declare that they have no conflicts of interest.

References

[1] C. Steele, "The finite beam with a moving load," *Journal of Applied Mechanics*, vol. 34, no. 1, pp. 111–118, 1967.

[2] E. Touti and A. P. Chobar, "Utilization of AHP and MCDM integrated methods in urban project management (A case study for eslamshahr-tehran)," *International journal of industrial engineering and operational research*, vol. 2, no. 1, pp. 16–27, 2020.

[3] L. Fryba, *Vibration of Solids and Structures under Moving Loads*, Springer Science and Business Media, Berlin, Germany, 3 edition, 1999.

[4] L. Fryba, S. Nakagiri, and N. Yoshikawa, "Stochastic finite elements for a beam on a random foundation with uncertain damping under a moving force," *Journal of Sound and Vibration*, vol. 163, no. 1, pp. 31–45, 1993.

[5] Y. H. Chen and Y. H. Huang, "Dynamic stiffness of infinite Timoshenko beam on viscoelastic foundation in moving co-ordinatefinite Timoshenko beam on viscoelastic foundation in moving coordinate," *International Journal for Numerical Methods in Engineering*, vol. 48, no. 1, pp. 1–18, 2000.

[6] L. Andersen, S. R. Nielsen, and P. Kirkegaard, "Finite element modelling of infinite Euler beams on Kelvin foundations exposed to moving load in convected co-ordinates," *Journal of Sound and Vibration*, vol. 241, no. 4, pp. 587–604, 2001.

[7] C. Koh, J. S. Y. Ong, D. K. H. Chua, and J. Feng, "Moving element method for train-track dynamics," *International Journal for Numerical Methods in Engineering*, vol. 56, no. 11, pp. 1549–1567, 2003.

[8] M. T. Tran, K. K. Ang, and V. H. Luong, "Vertical dynamic response of non-uniform motion of high-speed rails," *Journal of Sound and Vibration*, vol. 333, no. 21, pp. 5427–5442, 2014.

[9] P. M. Mathews, "Vibration of a beam on elastic foundation," *ZAMM - Zeitschrift für Angewandte Mathematik und Mechanik*, vol. 38, no. 3-4, pp. 105–115, 1958.

[10] L. Jezequel, "Response of periodic systems to a moving load," *Journal of Applied Mechanics*, vol. 48, no. 3, pp. 613–618, 1981.

[11] K. Ono and M. Yamada, "Analysis of railway track vibration," *Journal of Sound and Vibration*, vol. 130, no. 2, pp. 269–297, 1989.

[12] A. Trochanis, R. Chelliah, and J. Bielak, "Unified approach for beams on elastic foundations under moving loads," *Journal of Geotechnical engineering*, vol. 113, no. 8, pp. 879–895, 1987.

[13] F. F. Calım, "Forced vibration of curved beams on two-parameter elastic foundation," *Applied Mathematical Modelling*, vol. 36, no. 3, pp. 964–973, 2012.

[14] J. Dai, M. Han, and K. K. Ang, "Moving element analysis of partially filled freight trains subject to abrupt braking," *International Journal of Mechanical Sciences*, vol. 151, pp. 85–94, 2019.

[15] V. Nguyen and D. Duhamel, "Finite element procedures for nonlinear structures in moving coordinates. Part 1: infinite bar under moving axial loads," *Computers and Structures*, vol. 84, no. 21, pp. 1368–1380, 2006.

[16] V. Nguyen and D. Duhamel, "Finite element procedures for nonlinear structures in moving coordinates. Part II: infinite beam under moving harmonic loads," *Computers and Structures*, vol. 86, no. 21-22, pp. 2056–2063, 2008.

[17] T. P. Nguyen, D. T. Pham, and P. Hoang, "A new foundation model for dynamic analysis of beams on nonlinear foundation subjected to a moving mass," *Procedia Engineering*, vol. 142, pp. 166–173, 2016.

[18] G. Kouroussis and O. Verlinden, "Prediction of railway ground vibrations: a," *Soil Dynamics and Earthquake Engineering*, vol. 69, pp. 220–226, 2015.

[19] P. A. Ferreira and A. López-Pita, "Numerical modelling of high-speed train/track system for the reduction of vibration levels and maintenance needs of railway tracks," *Contents lists available at ScienceDirect Construction and Building Materials*, vol. 79, pp. 14–21, 2015.

[20] J. A. Zakeri and H. Xia, "Sensitivity analysis of track parameters on train-track dynamic interaction," *Journal of Mechanical Science and Technology*, vol. 22, no. 7, pp. 1299–1304, 2008.

[21] V. Sarvestan, H. R. Mirdamadi, and M. Ghayour, "Vibration analysis of cracked Timoshenko beam under moving load with constant velocity and acceleration by spectral finite element method," *International Journal of Mechanical Sciences*, vol. 122, pp. 318–330, 2017.

[22] R. U. A. Uzzal, R. B. Bhat, W. Ahmed, and W. Ahmed, "Dynamic response of a beam subjected to moving load and moving mass supported by Pasternak foundation," *Shock and Vibration*, vol. 19, no. 2, pp. 205–220, 2012.

[23] H. Hua, M. Qiu, and Z. Liao, "Dynamic analysis of an axially moving beam subject to inner pressure using finite element method," *Journal of Mechanical Science and Technology*, vol. 31, no. 6, pp. 2663–2670, 2017.

[24] G. Mei, C. Yang, S. Liang et al., "A reduced time-varying model for a long beam on elastic foundation under moving loads," *Journal of Mechanical Science and Technology*, vol. 32, no. 9, pp. 4017–4024, 2018.

[25] A. Jahangiri, N. K. A. Attari, A. Nikkhoo, and Z. Waezi, "Nonlinear dynamic response of an Euler–Bernoulli beam under a moving mass–spring with large oscillations," *Archive of Applied Mechanics*, vol. 90, no. 5, pp. 1135–1156, 2020.

[26] H. D. Phadke and O. R. Jaiswal, "Dynamic response of railway track resting on variable foundation using finite element method," *Arabian Journal for Science and Engineering*, vol. 45, no. 6, pp. 4823–4841, 2020.

[27] D. Froio, E. Rizzi, F. M. Simões, and A. Pinto da Costa, "Critical velocities of a beam on nonlinear elastic foundation under harmonic moving load," *Procedia Engineering*, vol. 199, pp. 2585–2590, 2017.

[28] E. Looi and F. Arbabi, "Stability and dynamic response of railroad tracks under stochastic loads," vol. 2, M.S. Thesis, 1987.

[29] F. Arbabi, A. Sherbourne, and H. El-Ghazaly, "Strength and deflection of railway tracks -I: probabilistic finite element analysis," *Computers and Structures*, vol. 39, no. 1-2, pp. 9–21, 1991.

[30] F. Li and F. Arbabi, "Stability and dynamic response of railroad tracks under stochastic loads," vol. 1, M.S. thesis, 1987.

[31] F. Arbabi and C. U. Loh, "Reliability analysis of railroad tracks," *Journal of Structural Engineering*, vol. 117, no. 5, pp. 1435–1447, 1991.

[32] M. Abolghasemian, A. P. Chobar, M. AliBakhshi, A. Fakhr, and S. Moradi, "Delay scheduling based on discrete-event simulation for construction projects," *Iranian Journal of Operations Research*, vol. 12, no. 1, pp. 49–63, 2021.

[33] F. Arbabi, "Variational formulation of rail overturning, Part 4, structural dynamics, systems identification. Computer amplifications. Shock and vibration," *Bulletin*, vol. 47, pp. 149–154, 1977.

[34] *National Iranian Trade Journal Number 301*, Public Technical Characteristics of Superstructure of railroad, Tehran, Iran, 2005.

[35] W. McGuire, R. Gallagher, and R. Ziemian, *Matrix Structural Analysis*, John Wiley and Sons. Inc, New York, NY, USA, 2000.

[36] A. V. Metrikine and H. A. Dieterman, "Instability of vibrations of a mass moving uniformly along an axially compressed beam on a viscoelastic foundation," *Journal of Sound and Vibration*, vol. 201, no. 5, pp. 567–576, 1997.

[37] S. Timoshenko, *Strength of Materials Part II: Advanced Theory and Problems*, Nine printing, van Nostrand, New York, NY, USA, 2 edition, 1940.